Russian Journal of Electrochemistry, Vol. 36, No. 5, 2000, pp. 457–464. Translated from Elektrokhimiya, Vol. 36, No. 5, 2000, pp. 517–525.

Palladium Electrodeposits: Dependence of Structure and Sorption Properties on the Deposition Potential

M. Yu. Rusanova, G. A. Tsirlina, O. A. Petrii, T. Ya. Safonova, and S. Yu. Vasil'ev

Moscow State University, Vorob'evy gory, Moscow, 119899 Russia

Received April 5, 1999

Abstract—A series of Pd electrodeposits (edPd) on Pt substrates is prepared at deposition potentials of –0.05 to 0.55 V with respect to a reversible hydrogen electrode in 0.5 M H_2SO_4. Their nanostructure is characterized by scanning tunneling microscopy. The size distribution of particles is estimated, and dependences of its maximum and half width on the deposition potential are determined. A comparative coulometric study of adsorption of copper and oxygen on edPd shows that real surface areas determined from these data substantially differ. The average size of particles for edPd, estimated within the model of equal-size spheres, is shown to be incorrect. The assumption that particles in the deposits essentially coalesce is substantiated. It is shown that the equilibrium hydrogen content in the α and β hydrides is anomalously high for the deposits whose growth was accompanied by deep hydrogenation of Pd. At a given effective pressure, for the α-phase, this value is always substantially higher as compared with less defective materials. In the β-phase, the hydrogen concentration can be either lower or higher.

INTRODUCTION

The sorptive and catalytic properties of palladium electrodeposits (edPd) on platinum foil strongly depend on the deposition potential E_d [1–4]. The structural factors that determine this dependence were studied earlier by means of X-ray methods and electron microscopy with a micron resolution on edPd deposited at –0.05 and 0.25 V [2], whose properties were believed to differ most essentially. Later [3, 4], substantial differences were revealed in the composition of the hydride's α-phase for edPd deposited at –0.05, 0.25, and 0.40 V on Pt and carbon cloth. It was also confirmed that much higher concentrations of hydride in the α-phase can be obtained for dispersed palladium as compared with compact samples.

Palladium is a unique catalyst of oxidation and hydrogenation of organic substances. Moreover, in contrast to catalysts of other platinum metals, its activity is determined by structural peculiarities not only of adsorption but also sorption properties. In particular, the electrocatalytic hydrogenation in membrane reactors, which can operate effectively only with the membrane surface covered by dispersed palladium, shows a considerable promise. The problem of a directed synthesis of active and selective catalytic edPd can be solved only by thoroughly studying the materials prepared under strictly controlled conditions and elucidating a correlation between structural features (average size of deposit particles, width of size distribution, structure of intergrain boundaries, texture) and the most important properties of Pd materials (parameters of hydrogen-sorption isotherms, surface coverage by different adatoms at different potentials, and the corresponding binding energies).

Having revealed such a correlation, one can elucidate on a new level how the fabrication conditions affect the catalyst's activity in concrete processes. In [5], a similar problem was solved for Pt/Pt using scanning tunneling microscopy (STM) and X-ray diffraction analysis.

EXPERIMENTAL

We studied edPd deposited on Pt in a potentiostatic mode at E_d ranging from –0.05 to 0.55 V.[1] The deposition was carried out from a 1 wt % $PdCl_2$ + 1 M HCl solution[2] in a cell with individed compartments. The substrate was placed inside the counter electrode, a smooth Pt cylinder of a high surface area. Substrates of Pt foil 0.1 to 0.2 mm thick with a surface area of 0.5 to 1 cm^2 were preliminarily treated in boiling aqua regia and alternately polarized cathodically and anodically in 0.1 M H_2SO_4. The deposit's weight m was determined from the weight difference of the electrode before and after Pd plating.

Before the measurements, edPd samples were purified by alternating anodic and cathodic polarization in 0.1 M H_2SO_4. The real surface areas of electrodes were determined using procedures based on the adsorption of copper [6] and oxygen [7] atoms. For this purpose, voltammetric curves were measured in 0.5 M H_2SO_4 (including solutions containing 0.1 M $CuSO_4$), from

[1] All potentials E are measured and presented with respect to a reversible hydrogen electrode (RHE) in 0.5 M H_2SO_4.

[2] The deposition solution pH (0.4) was lower than that of 0.5 M H_2SO_4 (0.5). The corresponding correction for the potential with respect to RHE in the deposition solution used in [1, 2] amounted to 6 mV.

1023-1935/00/3605-0457$25.00 © 2000 MAIK "Nauka/Interperiodica"

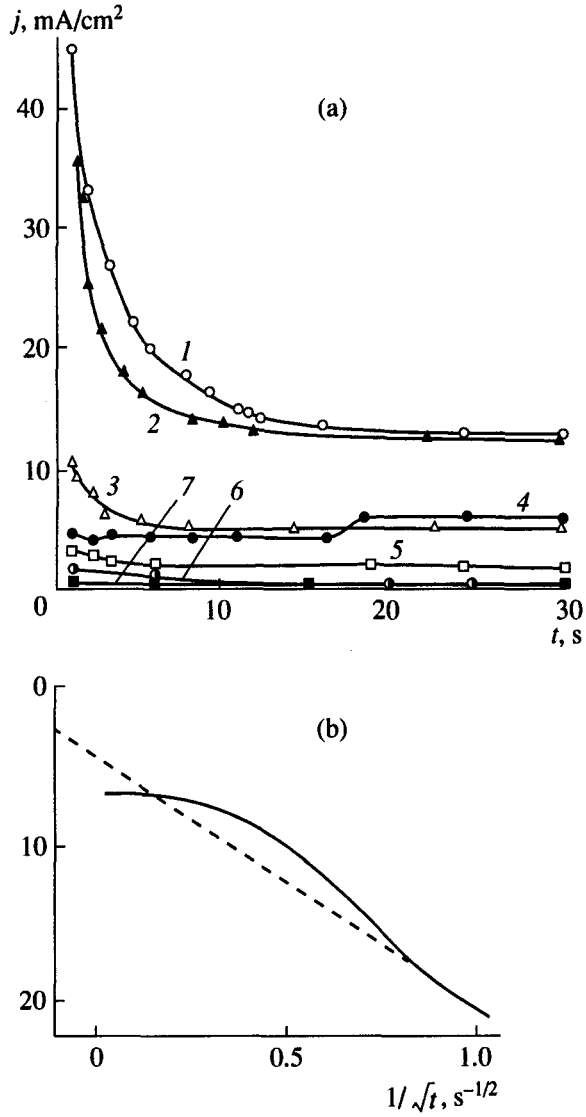

Fig. 1. (a) Initial sections of chronoamperograms for edPd deposited in potentiostatic mode at E_d of (*1*) 0.020, (*2*) 0.026, (*3*) 0.15, (*4*) 0.25, (*5*) 0.40, (*6*) 0.45, and (*7*) 0.55 V; (b) curve 2 of Fig. 1a plotted in the j vs. $\sqrt{t}$ coordinates, dashed line is an extrapolation to infinite time.

0.30 to 1.23 V, at potential scan rates v = 1–5 mV/s (in this interval, the estimated charges were independent of v). Fresh solutions were used in experiments with each electrode. When calculating real surface areas of electrodes we assumed that 420 μC/cm² is consumed for the desorption of monolayers of copper and oxygen adatoms; an accuracy of such a calculation could be estimated as 0.2 cm².

To study adsorption properties of edPd in the region of the α-phase hydride formation, we measured voltammetric curves in 0.5 M H_2SO_4 at v = 1–5 mV/s. For not-too-low hydrogen-sorption potentials, a complete hydrogen extraction was reached in the double-layer region. The time of hydrogen sorption under potentiostatic conditions was 20 min. The hydrogen content in the α-phase of Pd hydride was estimated in accordance with [3]. To determine the hydrogen content in the β-phase of Pd hydride in the region that precedes the α ⟷ β transition, equilibrium charging curves were measured via the procedure described in detail in [8, 9]. Before the measurements, the studied edPd was hydrogenated under potentiostatic conditions at 0.03 to 0.04 V for 6 h, with an inert gas being bubbled through the working electrode compartment. The saturation completeness was judged from the invariance of the potential after the circuit was opened. The current densities amounted to 0.1–1 mA per cm² of the geometric surface area.

In this study, solutions were prepared from H_2SO_4 (18 M), HCl (6 M), and water, all twice distilled. The solutions were deaerated by bubbling argon purified from oxygen traces. The electrochemical measurements were carried out in an automatic mode by using a PARC 273 potentiostat and an IBM 286 PC/AT computer with original software, in a three-electrode electrochemical cell with separated compartments.

The surface images were obtained by the STM method (design and characteristics of a LitScan2 microscope are described in [10]). Dry samples were scanned in air at a tunneling voltage of about 200 mV and tunneling currents of 100–200 pA. The image size ranged from 1400 by 1400 nm to 60 by 60 nm. In order to plot characteristic distributions, no less than 10 images of fine and medium scale were measured; the images were obtained in independent experiments when the probe was brought into contact with different points of a sample. The minimum particle size we managed to observe was no less than 5 nm. The error of the size determination during visual observation of the images did not exceed 10%. The approximation of the size distributions of particles by the normal distribution was carried out via the technique developed for characterization of edPt and described in [5].

RESULTS AND DISCUSSION

Palladium Electrodeposition Kinetics

Figure 1a shows initial regions of chronoamperograms of Pd deposition (current density j is normalized to geometrical surface area). In the initial period, the higher the overvoltage, the higher the current. Then, the current falls and reaches a constant value. At $E_d > 0.30$–0.40 V, the latter depends on the overvoltage (deposition under either kinetic or mixed control) and, at 0.10–0.30 V, is practically independent of E_d (deposition under diffusion control).

In the potential region of a hydride's β-phase formation, the deposition is characterized by the presence of an extended region of current delay and steady-state current values higher by a factor of 2–2.5 as compared with the preceding E_r region. An extrapolation of the

initial region to infinitely great times t in the j vs. $1/\sqrt{t}$ coordinates (Fig. 1b) gives the current values far exceeding zero. Figure 1b suggests that, in the course of deposition at great t, commensurate charges are consumed both in the Pd deposition itself and in the reduction of hydroxonium ions. Moreover, at the initial deposition stages, most of formed hydrogen adatoms recombine, and hydrogen molecules thus obtained move into solution. In subsequent, hydrogen atoms can also pass into the deposit's bulk. However, the accuracy of the extrapolation is not high, because the initial region corresponds to the hydrogen reaction on Pt, not on Pd, whereas, at great t values, the process occurs on Pd.

The suggested explanation agrees with the dependence of the current efficiency (CE) on E_d (Fig. 2): CE drops to ~40% precisely in the region of the $\alpha \longleftrightarrow \beta$ transition. On the whole, the data in Fig. 2 agree with similar data obtained in [1]. The decrease of CE at low overvoltages (low deposition rates), which was not studied earlier, can be explained by an increased contribution of the parallel oxygen reduction during deposition from aerated solutions. In the region of diffusion-controlled deposition, these contributions do not depend on E_d and are below 10% (Fig. 2).

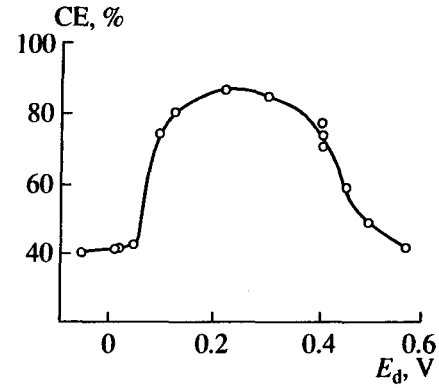

Fig. 2. Dependence of CE on E_d for Pd deposition.

Adsorption Properties of edPd

Figure 3a shows the specific surface area S of edPd determined from the adsorption of copper atoms as a function of E_d and also (dashed line) the surface-area curve estimated in [1] from the hydrogen adsorption at $E > 0.09$ V, in which a contribution of absorbed hydrogen in the hydride's α-phase is ignored. Later [6], it was reported that such a procedure can overestimate the S values by a factor of 7 to 8. The reasons for the appearance of a narrow maximum in curve *2* of Fig. 3a are considered in detail below. As a result of our study, we could more accurately plot the S vs. E_d dependences in the interval 0.05–0.30 V and, particularly, find the region of a smooth decrease in S with decreasing deposition overvoltage. Such a tendency is typical for the formation of metal deposits—at low growth rates more equilibrium crystals are formed.

Deposition of Pt from an H_2PtCl_6 solution is characterized by the opposite tendency (growth of S at low overvoltages), which was considered in [5] under the assumption about the disproportionation of an intermediate Pt(II) complex, which is the product of a two-electron reduction accumulated in the near-electrode layer. This additional contribution to the real surface area is caused by chemical deposition of Pt. In the case of electrodeposition of Pd(II), this situation is not observed.

Points *3* and *4* in Fig. 3a correspond to the literature data on S_{Cu} for edPd on Pt [4] and carbon cloth [12]. In the latter case, the deposit's structure probably depends on the nature of active centers of deposition. The reasons for the deviations from the data of [4] for edPd/Pt

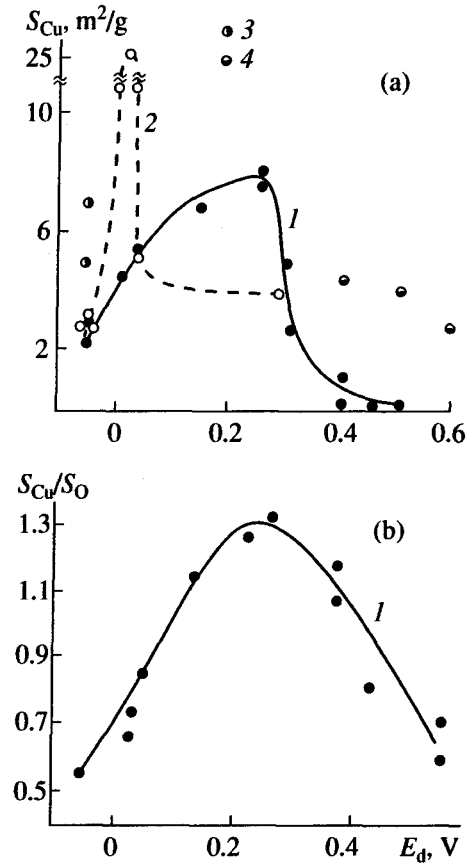

Fig. 3. The E_d dependences of (a) specific surface area of Pd and (b) ratio of surface areas by copper and oxygen: (*1*) data of this work; (*2*) data of [1], estimate by hydrogen desorption; (*3*) data of [4], (*4*) data of [12] for Pd on carbon cloth; see details in text.

are less evident. In particular, at $E_d = -0.05$ V, the cell's geometry may play a significant role in the Pd deposition, due to the parallel formation of hydrogen bubbles.

The ratio of real surface areas determined from the adsorption of copper and oxygen reveals a pronounced dependence on E_d (Fig. 3b). At $E_d < 0.10$ and $E_d > 0.40$ V, $S_{Cu}/S_O < 1$, which can be associated with overrated S_O during a coulometric analysis of the anodic

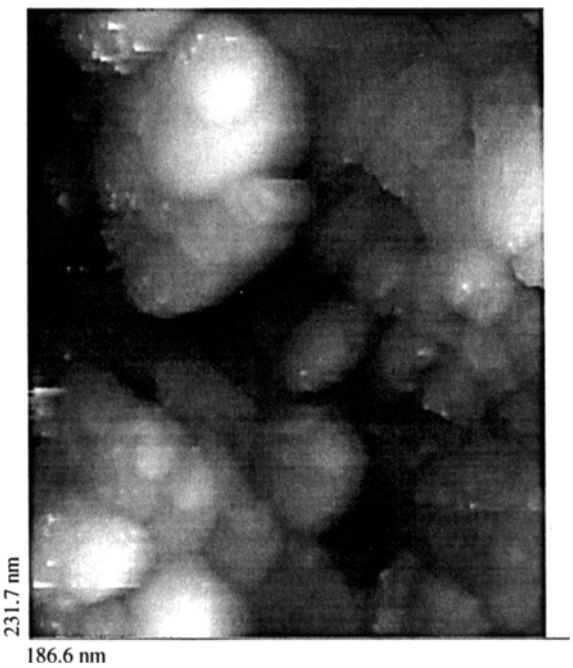

Fig. 4. Typical STM image of Pd/Pt surface.

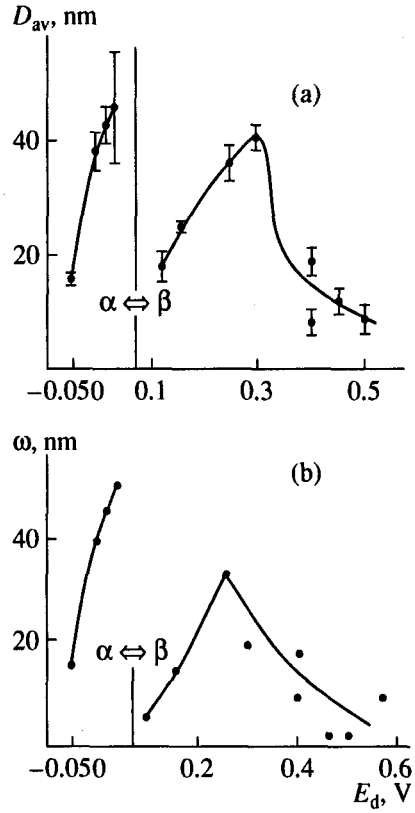

Fig. 5. (a) Position of maximum and (b) distribution half width as functions of E_d, plotted from STM data.

voltammetric curves, due to a possible contribution made by the Pd dissolution currents [13]. The ratios $S_{Cu}/S_O > 1$ can be explained by assuming that the surfaces of deposits obtained at medium overvoltages have some specific (for example, textured) areas which selectively adsorb anomalously high copper amounts. This assumption is corroborated by the dependence of the height ratio of four characteristic copper-desorption peaks on E_d (in principle, individual peaks can be attributed to the copper desorption from areas of specific crystallographic orientations [14]). Another possible explanation involves a substantial dependence of the oxygen adatom formation rate on E_d; however, such a dependence was not observed in the studied interval of v.

Special properties of copper and oxygen adatoms on dispersed Pd and those of the edPd texture will be analyzed in a separate publication.

STM Studies of edPd

Figure 4 shows a typical STM image of edPd, which reveals spherical and ellipsoid-like formations with sufficiently wide size distributions. Histograms of the size distribution $\varphi(D)$, obtained by statistically processing the images, to an approximation, can be described by the normal distribution

$$\varphi(D) = \frac{A}{\omega\sqrt{\pi/2}}\exp\left[-\frac{(D-D_{av})^2}{\omega^2}\right], \qquad (1)$$

where D_{av} is the average diameter of particles which corresponds to the distribution maximum, ω is the distribution's half width, and A is a normalizing parameter which characterizes the area under the distribution curve. Both D_{av} and ω strongly depend on E_d, and these dependences correlate (Figs. 5a, 5b): the higher the average size of particles, the wider the distribution. For the potential region of the $\alpha \longleftrightarrow \beta$ transition, both dependences demonstrate discontinuities, which suggests the existence of some specific deposition mechanism at the β-phase potentials. Strictly speaking, it is not metal that crystallizes in this region, but an isostructural hydride for which different types of active centers can exist in both initial and secondary nucleation modes.

As compared with edPt [5], edPd are characterized by substantially wider size distributions. For this reason, the consideration of size deviations of particles when analyzing the surface area (first of all, the contribution made by particles of extreme sizes) for edPd acquires new significance. Figure 6a shows experimental (curve *1*) and calculated (curve *2*) dependences of the average particle size on E_d. The calculation was done in terms of the model of equal-size spheres: $D_{av} = 6m/S\rho$, where ρ is the Pd density. The difference between curves *1* and *2* is particularly great at low overvoltages. This is also illustrated by Fig. 6b, in which curve *2* is plotted with the surface-area values esti-

mated with the procedure described in [5], using parameters of a size distribution under an assumption that the size distribution of spherical particles throughout the deposit's layers is the same as in the external (immediately observed) layer. The model of an acicular deposit was also considered, in which the observed size distribution of particles corresponds to diameters of the bases of high vertical cylinders normal to the surface (curve *3*, Fig. 6b). For the high-overvoltage region, an adequate agreement is achieved between experimental and calculated results; however, in a wide E_d region, the calculation substantially overrates S values. The deviations are especially high at $E_d > 0.35$–0.40 V, which corresponds to the kinetic (or mixed) control over the nucleation and growth. Apparently, when the edPd growth is slow, optimum conditions are realized for a complete or partial coalescence of particles and, consequently, the surface-screening effects are manifested stronger.

The data of Figs. 5a and 6b suggest that quantities D_{av} and S for edPd do not correlate, and the effects of coalescence (and/or screening of narrow pores) are largely responsible for the dispersion. From Fig. 6b, we conclude that the coalescence is less pronounced for edPd formed in the β-phase region. In this region, characteristic sizes of particles may be determined by the embrittlement of crystals during the hydrogen sorption. Such a nonequilibrium embrittlement ensures the presence of solution-permeable pores between particles.

Despite a substantial decrease in D_{av} as E_d changes from –0.05 to 0.05 V, the estimated S values are practically the same for this interval. This is due to the compensating effect of the difference in the distribution width. Note also that a comparative analysis similar to that shown in Fig. 6b with the use of S_O instead of S_{Cu} leads to the same conclusions. Moreover, differences between experimental and calculated data for the β-phase potentials turn out to be even smaller than in Fig. 6b.

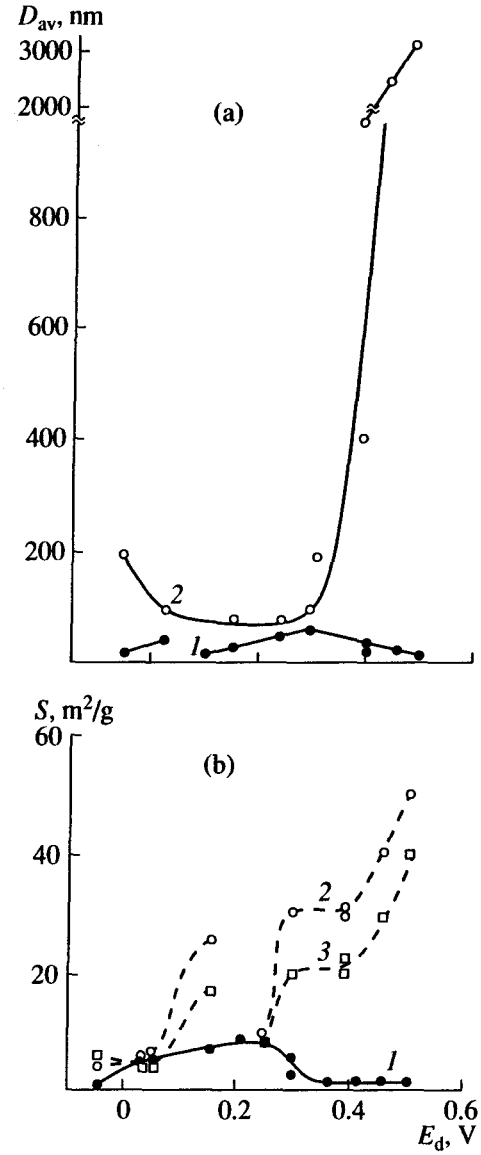

Fig. 6. (a) Average size of particles in deposits and (b) specific surface areas, as functions of E_d: (*1*) experimental, (*2a*) calculated with the equal-sphere model from the real surface area by copper, (*2b*) calculated via the procedure [5] for spherical particles, and (*3b*) calculated for acicular deposits.

Absorption Properties of edPd

When comparing sorption properties of edPd, we restricted ourselves to the case of hydride compositions corresponding to $E_r < 0.1$ V. This means that we did not analyze in detail the sorption-isotherm sections corresponding to low effective pressures p_{H_2} (calculated for each saturation potential via the Nernst equation).

In contrast to the curves obtained earlier [9], the equilibrium charging curves were recorded by passing a charge increased in small increments even in the region of the α-phase formation. This allowed us to extend, for the first time, the interval of studied equilibrium compositions of this phase to the region of the α ⟷ β transition plateau.

A comparison of the results of a potentiodynamic extraction with those of equilibrium measurements shows that the first procedure at $v = 1$ mV/s provides the equilibrium hydrogen extraction only at saturation potentials exceeding 0.08–0.085 V. Figure 7a shows equilibrium sections of characteristic isotherms. In the studied interval, they do not obey a linear dependence on $\sqrt{p_{H_2}}$, and their slopes increase with the H/Pd atomic ratio. By extrapolating the lower linear sections of isotherms to $p_{H_2} = 0$, we obtained nonzero H/Pd varying in the interval of ~0.001–0.02 practically for all studied samples. In terms of a formal consideration [15], which was used earlier for analyzing properties of the hydride's α-phase for defective Pd materials, these values correspond to the concentration r_t^0 of defective

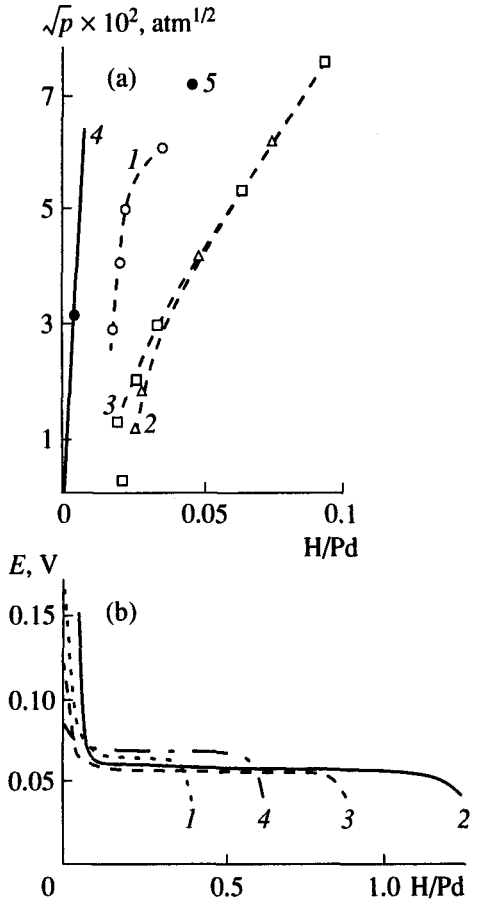

Fig. 7. Hydrogen sorption isotherms for Pd/Pt in the regions of (a) concentrated α phase and (b) phase transition, obtained at E_d of (*1*) 0.05, (*2*) 0.026, (*3a*) 0.04, (*3b*) 0.02, (*4b*) 0.30, and (*5a*) 0.55 V; curve *4a* refers to compact Pd.

positions in a deformed lattice,

$$\text{H/Pd} = r_t^0 \frac{\sqrt{p_{H_2}}}{K + \sqrt{p_{H_2}}} + \frac{\sqrt{p_{H_2}}}{K_S}, \qquad (2)$$

where K_S is the Siverts constant for defectless regions, and K is a constant of the equilibrium between hydrogen in defective and defectless positions normalized to K_S. As a rule, K_S values, determined experimentally at low $\sqrt{p_{H_2}}$, ranged from 2 to 6 atm$^{0.5}$, which agrees with characteristic values for defective materials studied earlier [3, 4, 12, 15, 16].[3] However, at higher $\sqrt{p_{H_2}}$, which were ignored in the aforementioned works, K_S formally decreases to <1 atm$^{0.5}$ and demonstrates a tendency to a further decrease.

[3] A correction for the contribution of adsorbed hydrogen [16], which was significant in describing quantitatively diluted hydrides, is irrelevant in the pressure interval under consideration. It was introduced by using the potential dependence of the hydrogen coverage measured on Pd blacks [16], which apparently corresponded to H/Pd values somewhat underrated (by no more than 1 to 2%).

Due to wide differences between slopes of the H/Pd vs. $\sqrt{p_{H_2}}$ dependences, it is not quite correct to compare H/Pd values for different edPd at a constant pressure. Moreover, reproducibility of absorption characteristics for the same E_d is substantially lower as compared with the aforementioned structural and adsorption characteristics. This is easily explained by the fact that the formation of nonequilibrium defects in the material bulk during electrodeposition is determined by many factors that are difficult to control [11]. However, we can find some tendencies in the effect of E_d on the sorption behavior.

For edPd obtained at medium E_d of 0.25–0.40 V, the values of r_t^0 are always lower and the K_S values are higher as compared with edPd prepared during the formation of a concentrated hydride. The deposits obtained at $E_d = 0.55$ V are characterized by H/Pd equal to the hydrogen concentration in polycrystalline Pd (point *5* and curve *4* in Fig. 7a). However, in this case, a more detailed study of a sorption isotherm is limited by small thickness of deposits. We assume that a smooth material formed at low overvoltages has a practically equilibrium lattice which includes its intergrain boundaries.

The samples deposited at 0.020 and 0.026 V, which demonstrated [1] anomalously high specific surface areas with respect to hydrogen adsorption (curve *2*, Fig. 3a), are characterized by very high H/Pd. Particularly, at a saturation potential of 0.090 V, from which the measurements started [1], the values of H/Pd always exceeded 0.03. For these deposits, the effective surface area estimated as in [1] is 20–24 m^2/g, which is close to the maximum values presented in [1] and differs from S_{Cu} by a factor of 4 to 5.

The equilibrium potential of the α ⟷ β transition also depends on E_d (Fig. 7b) and amounts to 0.060–0.062 V for edPd formed in the β-phase region and 0.065–0.072 V for all other deposits (the accuracy of determining the "plateau" potential in equilibrium measurements was 0.002 to 0.003 V, hence, the aforementioned difference is significant). In some cases, the region of α ⟷ β transition demonstrates additional plateaus, whose potentials differ by 0.002 to 0.003 V. Parameters of the H/Pd vs. $\ln p_{H_2}$ dependences, estimated from short sections of the sorption isotherms in the β-phase region, agree by and large with those found earlier [9, 17–19] for $E_d > 0.15$ V ($a = -11.1 \pm 1$, $b = 15.9 \pm 1.7$) and differ from them for E_d corresponding to the β-phase formation. The samples obtained in this potential region are characterized by highly anomalous compositions of the concentrated hydride: at $E_r = 0.04$ V, H/Pd is about 0.4 for $E_d = -0.05$ V (which agrees with [1] for the same E_d), whereas, for $E_d = 0.020$ and 0.026 V, H/Pd of ~0.9 and ~1.2, respectively, are reached under the same conditions. For most disperse and compact materials studied earlier [17–19] and for the deposits

Characteristics of three types of edPd/Pt

Interval of E_d, V, and nucleation mechanism	S_{Cu}/S_O	Degree of particle coalescence	Properties of α-hydride as compared to compact materials	Properties of β-hydride as compared to compact materials
<0.40–0.45, kinetic control	<1	very high	close	identical
0.06–0.10...0.40–0.45 diffusion control	>1	detectable	higher	
<0.06 deposition and hydride formation	<1	hardly detectable	substantially higher	substantially different

obtained in this work at low and medium overvoltages, the hydrogen concentration in Pd is 0.62–0.64 under the same conditions. Evidently, the anomalously high concentrations of both α and β hydrides for the samples with E_d of about 0.02 V result from an anomalous structure of defective regions in these materials. A comprehensive analysis of these anomalous deposits requires additional experimental studies. Here, we merely make some conclusions on the basis of our study.

The Siverts law underlying the consideration [15], in its simplified form (which can be applied only to very diluted hydride phases [19]) assumes the absence of long-range effects. Therefore, for a small number of defective positions, at least after their saturation (H/Pd = r_i^0) in some pressure interval, a linear dependence with a slope K_S^{-1} equal to that known for defectless (large-crystal, annealed) Pd should be observed (at about 12 $atm^{0.5}$ when at room temperature [19]).

As follows from our data, the significantly lower K_S values usually determined by a linear approximation of the isotherms' sections at $\sqrt{p_{H_2}} < 0.03$ to 0.04 $atm^{0.5}$ do not arise from some error associated with the narrowness of the considered interval. On the contrary, when the interval is extended to 0.08 $atm^{0.5}$, the K_S values are even lower. We assume that, for defective materials studied in [3, 4, 12, 15, 16] and in our work, the defectless regions identical to an equilibrium lattice are either absent or present in concentrations substantially higher than r_i^0 and, hence, the contribution of equilibrium regions is not predominant up to potentials of the α ⟷ β transition.

For a wide diversity of Pd materials, sorption isotherms in the β-phase are described by the same relationships [17–19], which makes it possible to assign relevant parameters of the H/Pd vs. $\ln p_{H_2}$ dependences to a defectless lattice. Evidently, at low volume contents of defectless positions, their contributions to substantial values of H/Pd for concentrated hydrides are difficult to reveal experimentally. That is why the aforementioned substantial deviations of concentrations in the β-phase both to greater and lower values presumably indicate a small (and even zero) bulk content of defectless lattice fragments in the materials. For a deposit obtained at E_d = –0.05 V, numerous defective positions probably tend to form concentrated hydrides at higher pressures as compared with an equilibrium Pd lattice, whereas, for deposits prepared at E_d = 0.020 and 0.026 V, this is true for lower pressures.

The constant K in (2) is independent of the hydride composition. This fact suggests that the chemical potential of hydrogen dissolved in defective positions is independent of its concentration, whereas the approach to a linear H/Pd vs. $\ln \sqrt{p_{H_2}}$ dependence is believed to confirm the limiting occupation of these positions. In fact, if defective positions are arranged in compact groups (for example, in the vicinity of intergrain boundaries), interaction of hydrogen atoms in neighboring positions inevitably affects the effective value of K, which is taken into account in the Siverts law by introducing an H/Pd-dependent factor. Considering such a dependence of K on the hydrogen concentration is similar to considering n defective regions in the material bulk with volume fractions N_i. The variation of K with the composition even at a small number of dislocation defects was confirmed in [20] by analyzing an equilibrium between hydrogen in defective and defectless positions, and it is precisely this model that lies in the basis of our consideration [15]. In the future, it seems worthwhile to analyze complicated sorption isotherms by taking into account additive contributions of different kinds of regions on the basis of existing classic relationships [19], i.e.,

$$\text{H/Pd} = \sqrt{p_{H_2}} \sum_{i=1}^{n} \frac{N_i}{K_i + \sqrt{p_{H_2}}} \quad (\alpha \text{ phase}),$$

$$\text{H/Pd} = \sum_{i=1}^{n} (a_i + b_i \ln p_{H_2}) \quad (\beta \text{ phase}), \qquad (3)$$

$$\sum_{i=1}^{n} N_i = 1.$$

The first of these relationships generalizes equation (2) for the cases where the concentration of defective positions is almost unity and also for arbitrary pressure intervals and space distributions of defects. This allows us to propose a new procedure for analyzing experimental data in the coordinates (H/Pd)/$\sqrt{p_{H_2}}$ vs. p_{H_2} and assess (under the assumption about single-type defec-

tive sites) the value of K for the defective region at small coverages (in the absence of interaction between neighboring hydrogen atoms). According to our estimates based on available experimental data, the relevant values amount to no more than 0.02–0.05 $atm^{0.5}$, which is below those obtained by a fitting analysis over the whole pressure interval [15]. This result unambiguously confirms the significance of interactions in limited volumes of defective regions, i.e., suggests that edPd exhibits not individual defects separated by equilibrium lattice regions, but compact defective regions.

CONCLUSION

Summarizing the results, we claim the existence of three different types of electrodeposits which can be prepared in different overvoltage domains. The revealed anomalous sorption properties are of special significance for catalytic applications. The possibility of generation of highly reproducible special types of defective bulk positions with high-energy hydrogen bonds is of fundamental importance.

Palladium hydrides represent a very promising model system for studying equilibrium in nonstoichiometric defective phases and for considering problems of electrochemical thermodynamics in nonstoichiometric systems.

ACKNOWLEDGMENTS

This work was supported by the Russian Foundation for Basic Research, project no. 99-03-32 341.

REFERENCES

1. Podlovchenko, B.I., Petukhova, R.P., Kolyadko, E.A., and Lifshits, A.D., *Elektrokhimiya*, 1976, vol. 12, p. 813.
2. Gamburg, Yu.D., Petukhova, R.P., Lifshits, A.D., *et al.*, *Elektrokhimiya*, 1979, vol. 15, p. 1875.
3. Kolyadko, E.A., Shigan, Lu., and Podlovchenko, B.I., *Elektrokhimiya*, 1992, vol. 28, p. 385.
4. Podlovchenko, B.I., Kolyadko, E.A., and Shigan, Lu., *J. Electroanal. Chem.*, 1995, vol. 399, p. 21.
5. Petrii, O.A., Tsirlina, G.A., Pron'kin, S.N., *et al.*, *Elektrokhimiya*, 1999, vol. 35, p. 12.
6. Maksimov, Yu.M., Lapa, A.S., and Podlovchenko, B.I., *Elektrokhimiya*, 1989, vol. 25, p. 712.
7. Breiter, M.W., *J. Electroanal. Chem.*, 1977, vol. 81, p. 275.
8. Tsirlina, G.A., Rusanova, M.Yu., and Petrii, O.A., *Elektrokhimiya*, 1993, vol. 29, p. 469.
9. Tsirlina, G.A., Rusanova, M.Yu., Roznyatovskii, V.A., and Petrii, O.A., *Elektrokhimiya*, 1995, vol. 31, p. 25.
10. Vasil'ev, S.Yu. and Denisov, A.V., *Zh. Tekh. Fiz.*, 2000, vol. 70, p. 100.
11. Gamburg, Yu.D., *Elektrokhimicheskaya kristallizatsiya metallov i splavov* (The Electrochemical Crystallization of Metals and Alloys), Moscow: Yanus-K, 1997.
12. Shigan, Lu., Kolyadko, E.A., and Podlovchenko, B.I., *Elektrokhimiya*, 1993, vol. 29, p. 465.
13. Rand, D. and Woods, R., *J. Electroanal. Chem.*, 1972, vol. 35, p. 209.
14. Chierchie, T. and Mayer, C., *Electrochim. Acta*, 1988, vol. 33, p. 341.
15. Bucur, R.V., *J. Mater. Sci.*, 1987, vol. 22, p. 1402.
16. Shigan, Lu., Kolyadko, E.A., and Podlovchenko, B.I., *Elektrokhimiya*, 1993, vol. 29, p. 461.
17. Fedorova, A.I. and Frumkin, A.N., *Zh. Fiz. Khim.*, 1953, vol. 27, p. 247.
18. Perminov, P.S., Orlov, A.A., and Frumkin, A.N., *Dokl. Akad. Nauk SSSR*, 1952, vol. 84, p. 749.
19. *Hydrogen in Metals*, Alefeld, G. and Voelkl, J., Eds., Berlin: Springer, 1978.
20. Oriani, R.A., *Acta Metall. Mater.*, 1970, vol. 18, p. 147.